MoO_3/Ag/Al/ZnO intermediate layer for inverted tandem polymer solar cells*

Qing Jian(卿 健), Zhong Zhen-Feng(钟镇锋), Liu Yong(刘 勇), Li Bao-Jun(李宝军), and Zhou Xiang(周 翔)†

State Key Lab of Optoelectronic Materials and Technologies, School of Physics and Engineering, Sun Yat-Sen University, Guangzhou 510275, *China*

(Received 18 June 2013; revised manuscript received 13 August 2013; published online 24 January 2014)

We report an MoO_3/Ag/Al/ZnO intermediate layer connecting two identical bulk heterojunction subcells with a poly(3-hexylthiophene) and [6,6]-phenyl-C61-butyric acid methyl ester (P3HT and PCBM) active layer for inverted tandem polymer solar cells. The highly transparent intermediate layer with an optimized thickness realizes an Ohmic contact between the two subcells for effective charge extraction and recombination. A maximum power conversion efficiency of 3.76% is obtained for the tandem cell under 100 mW/cm^2 illumination, which is larger than that of a single cell (3.15%). The open-circuit voltage of the tandem cell (1.18 V) approaches double that of the single cell (0.61 V).

Keywords: polymer solar cell, inverted structure, tandem solar cell, intermediate layer

PACS: 88.40.jr, 88.40.–j, 84.60.Jt **DOI:** 10.1088/1674-1056/23/3/038802

1. Introduction

Polymer solar cells (PSCs) have received great attention in recent years due to their mechanical flexibility, light weight, and potential for low-cost manufacturing.[1–5] Remarkable progress has been achieved in recent years on bulk heterojunction (BHJ) polymer-fullerene solar cells with power conversion efficiencies (PCEs) between 4% and 5% for poly(3-hexylthiophene) and [6,6]-phenyl-C61-butyric acid methyl ester (P3HT:PCBM)[6,7] and up to 9% for a new generation of low-bandgap polymers.[8,9] However, the efficiency is still limited by the low carrier mobility and the narrow absorption spectra of the polymers. Tandem solar cells consisting of two or more subcells with complementary absorption spectra can further increase the efficiency. In tandem PSCs, the intermediate layers are crucial and should provide an Ohmic contact to facilitate the efficient recombination of opposite charge carriers from the top and the bottom subcells.[10] Moreover, for tandem cells with polymer based subsequent subcells, the intermediate layers should protect the bottom cell and be wettable for the processing of the top cell. So far, quite a few intermediate layers have been reported and reviewed,[10–12] such as Al/MoO_3,[13] TiO_x/PEDOT:PSS,[14] ZnO/PEDOT:PSS,[15] MoO_3/Ag/Al/Ca,[16] MoO_3/Al/ZnO-d,[17] and PEDOT:PSS/ZnO.[4,18,19]

On the other hand, the conventional BHJ PSCs with an active layer sandwiched between an aluminum cathode and a PEDOT:PSS layer on the top of an indium tin oxide (ITO) substrate have some drawbacks in spite of the high PCEs. The air-sensitive, low-work-function aluminum cathode and the acidic and hygroscopic nature of the PEDOT:PSS are the most common causes for instability in the conventional device architecture.[20–23] In addition, it has been reported that the vertical phase separation of the active layer in BHJ PSCs exhibits the enrichment of the donor and the acceptor components at the top and the bottom surfaces, respectively, which is unfavorable for charge transport in the conventional structure.[24] A very effective way to circumvent this problem was proposed with the so-called inverted structure.[25,26] In the inverted devices, the interface of ITO/PEDOT:PSS can be avoided and Al can be replaced with air-stable, high-work-function metals such as Au and Ag. A significant improvement in the air stability of the solar cells has been demonstrated.[27,28]

Therefore, both efficiency and stability of the solar cells could be improved by combining tandem and inverted structure together. This structure has been recently exemplified by Sun *et al.*[16] by using MoO_3/Ag/Al/Ca as the intermediate layer. However, the thermal evaporation of the active metal Ca complicated the fabrication process, which needed three evaporations in a vacuum and must be completed in a nitrogen environment.

Here, we replace the active Ca with a layer of ZnO nanoparticles and demonstrate a new intermediate layer of MoO_3/Ag/Al/ZnO for the inverted tandem PSCs. The stable and solution-processed ZnO nanoparticle layer simplifies the fabrication process greatly. For the MoO_3/Al/ZnO-d interme-

*Project supported by the National Basic Research Program of China (Grant No. 2012CB933704), the Doctoral Foundation of the Ministry of Education of China (Grant No. 20100171110025), and the State Key Laboratory of Optoelectronic Materials and Technologies, Sun Yat-Sen University, China (Grant No. 2010-RC-3-1).

†Corresponding author. E-mail: stszx@mail.sysu.edu.cn

© 2014 Chinese Physical Society and IOP Publishing Ltd

diate layer reported recently by Chou *et al.*,[17] the sol–gel ZnO-d layer usually has to be annealed at high temperature (over 200 °C) to remove the solvent,[27,29,30] while the annealing temperature of the layer of ZnO nanoparticles is comparably low (around 100 °C), which is better for the fabrication of tandem solar cells.[4,18,31]

2. Experimental details

The device structure of the inverted tandem PSCs is shown in Fig. 1(a). The tandem cells were fabricated on ITO-coated glass substrates with a sheet resistance of 50 Ω/□. The ITO glass substrates were ultrasonically cleaned in acetone, alcohol, and de-ionized water for 10 min sequentially, followed by a 10 min O_2 plasma treatment. A thin layer of ZnO nanoparticles from acetone, synthesized using the method introduced by Beek *et al.*,[32] was spin coated onto the ITO-coated glass, followed by annealing at 150 °C for 10 min. Then a blend solution of P3HT:PCBM (Echo Chemcial Co. Ltd., Taiwan) with a weight ratio of 1:1 in chlorobenzene (10 mg/mL) was spin coated to form the bottom active layer. MoO_3, Ag, and Al were subsequently thermally evaporated on the top of the bottom cell under high vacuum (6×10^{-4} Pa). The thicknesses of the thin films were monitored by a quartz thickness monitor. Another thin layer of ZnO nanoparticles (30 nm) was spin coated, followed by thermal annealing at 100 °C for 10 min to form the intermediate layer, i.e., MoO_3/Ag/Al/ZnO. Afterwards, the top active layer of P3HT:PCBM was spin coated on the intermediate layer. Finally, to complete the tandem solar cells, an MoO_3 buffer (10 nm) and an Ag anode (80 nm) were thermally evaporated (6×10^{-4} Pa). The post-annealing of the devices was performed at 130 °C for 10 min. All the spin coating and annealing treatments were done in an ambient environment. The effective area of the devices was around 9 mm^2. The layer thicknesses were calibrated with a Veeco Dektak 6M Stylus Profiler. The transmittance spectra of the samples were determined by depositing on a quartz and measuring with a Perkin Elmer-Lambda 750 UV/Vis/NIR spectrophotometer. Current density–voltage (J–V) characteristics were measured with a Keithley 236 source meter unit under 100 mW/cm^2 simulated AM1.5G illumination.

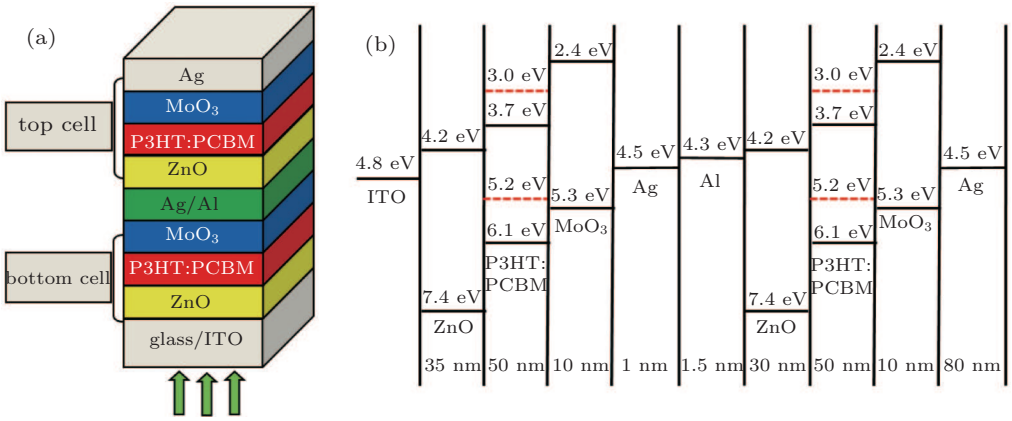


Fig. 1. (color online) (a) Device structure of the inverted tandem solar cell with MoO_3/Ag/Al/ZnO intermediate layer, (b) energy-level diagram of the tandem cell.

3. Results and discussion

Figure 1(b) illustrates the energy level diagram of the tandem cell, indicating the highest occupied molecular orbital (HOMO) energies and the lowest unoccupied molecular orbital (LUMO) energies of each layer, as well as the work functions of the conductive electrodes. By considering the transmittance and the work function, MoO_3 was chosen as the anode buffer layer for hole collection and a thin layer of ZnO nanoparticles was chosen as the cathode buffer layer for electron collection. The thickness of each layer in the MoO_3/Ag/Al/ZnO intermediate layer is also very important. The MoO_3 layer has to be thick enough to protect the bottom subcell, yet thin enough to avoid large voltage loss and high series resistance.[16,33] The Al layer can improve both the wettability and the electrical contact.[34] Without Al or with thinner Al (less than 1.5 nm), the top subcell could not be spin coated well. We also changed the sequence of Ag and Al to try the intermediate layer of MoO_3/Al/Ag/ZnO. However Ag at the top of Al decreases the wettability of the surface, leading to inferior film formation for the next spin coating. The J–V characteristics of the tandem solar cells with different thicknesses of Ag (0.5 nm, 1 nm, 1.5 nm) and Al (1.5 nm, 2 nm) are shown in Fig. 2 and the performances of the devices are summarized in Table 1. The optimal thicknesses of Ag and Al are 1 nm and 1.5 nm, respectively, and the corresponding best tandem cell shows a PCE of 3.76%.

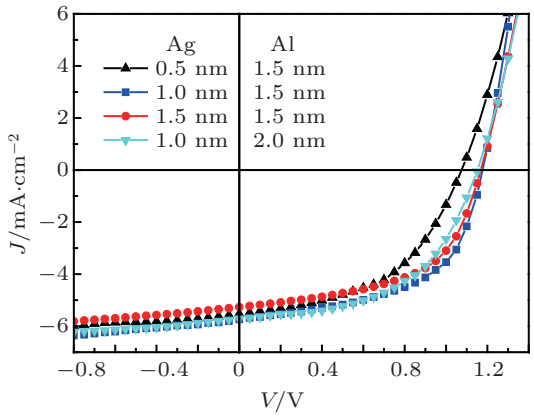


Fig. 2. (color online) The *J*–*V* characteristics of tandem solar cells with different thicknesses of Ag and Al.

Table 1. Performances of tandem solar cells with different thicknesses of Ag and Al.

Ag/nm	Al/nm	V_{oc}/V	J_{sc}/mA·cm^{-2}	FF/%	PCE/%
0.5	1.5	1.08	5.54	49.6	2.95
1	1.5	1.18	5.83	54.9	3.76
1.5	1.5	1.17	5.26	55.1	3.39
1	2	1.15	5.72	52.2	3.44

Figure 3 shows the absorption spectrum of the P3HT:PCBM film and compares the transmittances of different combinations of intermediate layers. The high transmittance almost exceeding 90% from 400 nm to 800 nm ensures the minimal optical loss. Compared with the transmittances of MoO_3 and MoO_3/Al/ZnO, the transmittance dip peaking of MoO_3/Ag/Al and MoO_3/Ag/Al/ZnO at 466 nm can attribute to the Ag nanocluster layer (1 nm) due to the localized surface plasmon resonance.[16,35,36]

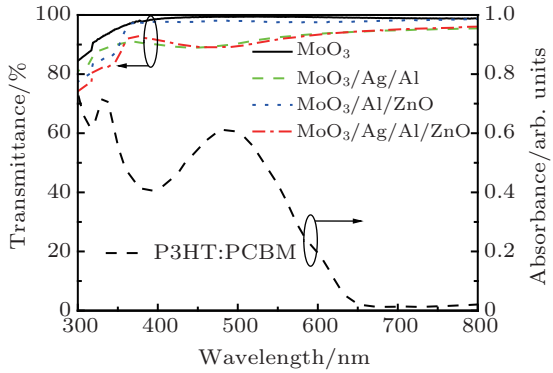


Fig. 3. (color online) The transmittance spectra of different intermediate layers and the absorption spectrum of the P3HT:PCBM film.

The *J*–*V* characteristics of the typical single and optimal tandem cell under illumination are shown in Fig. 4 and the performances of the devices are summarized in Table 2. The inverted single cell ITO/ZnO/P3HT:PCBM/MoO_3/Ag yields a PCE of 3.15%, with V_{oc} of 0.61 V, short-circuit current density J_{sc} of 9.05 mA/cm^2, and fill factor (FF) of 56.9%. The tandem cell ITO/ZnO/P3HT:PCBM/MoO_3/Ag/Al/ZnO/P3HT:PCBM/MoO_3/Ag yields a PCE of 3.76%, with V_{oc} = 1.18 V, J_{sc} = 5.83 mA/cm^2, and FF = 54.9%. The V_{oc} of the tandem cell approaches double that of the single cell, suggesting the effectiveness of the MoO_3/Ag/Al/ZnO intermediate layer. The J_{sc} decreases since identical materials (P3HT:PCBM) are used as the active layer for both subcells. However, the PCE of the tandem cell is higher. This may be due to the fact that the single cell has not achieved the best performance because of the relatively thin active layer (50 nm) and the thin active layer is favorable for tandem cells with identical subcells.[37]

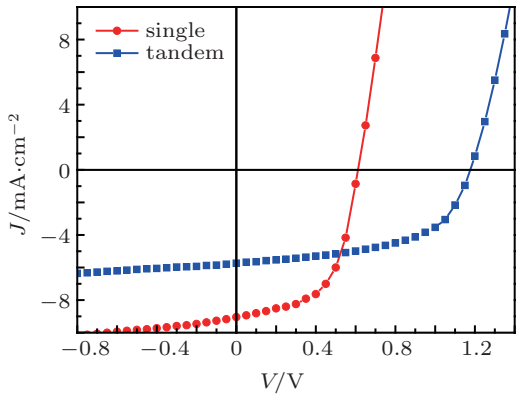


Fig. 4. (color online) The *J*–*V* characteristics of the single cell (ITO/ZnO/P3HT:PCBM/MoO_3/Ag) and the tandem cell using MoO_3/Ag/Al/ZnO as the intermediate layer.

Table 2. Performances of the inverted single and the tandem solar cells.

Cell	V_{oc}/V	J_{sc}/mA·cm^{-2}	FF/%	PCE/%
Single	0.61	9.05	56.9	3.15
Tandem	1.18	5.83	54.9	3.76

Figure 5 compares the *J*–*V* characteristics of the inverted tandem cells with different intermediate layers. The device with the MoO_3/Ag/Al/ZnO intermediate layer shows an excellent photovoltaic behavior, while the other two, without ZnO or Ag, exhibit much inferior performance. The s-shape *J*–*V* behavior near V_{oc} indicates a significant energy barrier for charge extraction or recombination at the intermediate layer while the lower photocurrent can be ascribed to the poor charge selectivity of the intermediate layer.[16,17,38] For the MoO_3/Ag/Al intermediate layer without ZnO, MoO_3 can simultaneously contact with both the top and the bottom active layers due to the ultrathin Ag/Al layer, which reduces the build-in potential of the top subcell. Thus, exciton separation and charge extraction of the top subcell cannot complete efficiently, resulting in a low photocurrent. The unbalanced charge injection into the intermediate layer results in the s-shape behavior and a lower V_{oc} of 0.70 V. For the MoO_3/Al/ZnO intermediate layer without Ag, the J_{sc} is close

to the regular tandem cell, indicating that there is no energy barrier for charge extraction. However, the low V_{oc} (0.95 V) and the s-shape curve suggest the existence of an energy barrier for charge recombination at the intermediate layer. This may be caused by the formation of an oxide layer (O deficient) at the interface of Al/ZnO due to air exposure of Al for the next spin coatings in an ambient environment. The insertion of a thin Ag layer between MoO_3 and Al can form an energy step with Al for efficient charge recombination of the electrons extracted from the top subcell through ZnO and the holes extracted from the bottom subcell through MoO_3.[16] So all four layers (MoO_3/Ag/Al/ZnO) are necessary and combine together to form an efficient intermediate interlayer.

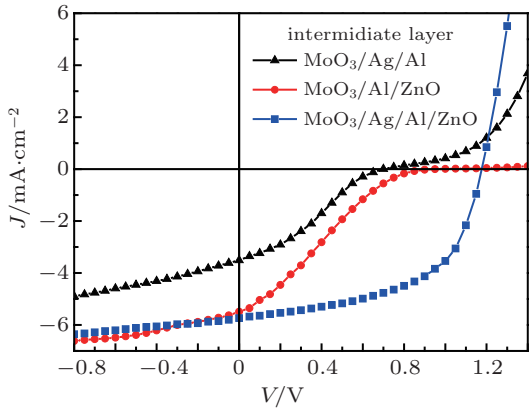


Fig. 5. (color online) Comparison of the J–V characteristics of the inverted tandem cells with different intermediate layers.

4. Conclusion

In conclusion, we have successfully presented the MoO_3/Ag/Al/ZnO intermediate layer which is physically strong to protect the underlying layer, optically transparent to minimize the optical loss, and electrically conductive to connect the top and the bottom subcells of the inverted tandem PSCs. With an optimal thickness, the V_{oc} of the tandem cell (1.18 V) approaches the double that of the single cell (0.61 V) and the tandem cell exhibits a PCE of 3.76%, which is larger than that of the single cell (3.15%). Further advances in efficiency can be expected when polymer materials with complementary absorption are used.

Acknowledgment

The authors would like to thank Miss Yang Yu-Zhao and Mr. Zhang Wen-Kai for technical support to synthesize the ZnO nanoparticles.

References

[1] Tang C W 1986 *Appl. Phys. Lett.* **48** 183
[2] Wu J, Guo X Y and Xie Z Y 2012 *Chin. Phys. Lett.* **29** 98801
[3] Liu X D, Zhao S L, Xu Z, Zhang F J, Zhang T H, Gong W, Yan G, Kong C, Wang Y S and Xu X R 2011 *Chin. Phys. B* **20** 68801
[4] Dou L, You J, Yang J, Chen C C, He Y, Murase S, Moriarty T, Emery K, Li G and Yang Y 2012 *Nature Photon.* **6** 180
[5] Feng Z H, Hou Y B, Shi Q M, Liu X J and Teng F 2010 *Chin. Phys. B* **19** 098601
[6] Reyes-Reyes M, Kim K, Dewald J, López-Sandoval R, Avadhanula A, Curran S and Carroll D L 2005 *Org. Lett.* **7** 5749
[7] Ma W, Yang C, Gong X, Lee K and Heeger A J 2005 *Adv. Funct. Mater.* **15** 1617
[8] He Z C, Zhong C M, Huang X, Wong W Y, Wu H B, Chen L W, Su S J and Cao Y 2011 *Adv. Mater.* **23** 4636
[9] He Z C, Zhong C M, Su S, Xu M, Wu H B and Cao Y 2012 *Nature Photon.* **6** 593
[10] Yuan Y, Huang J and Li G 2011 *Green* **1** 65
[11] Hadipour A, de Boer B and Blom P W M 2008 *Adv. Funct. Mater.* **18** 169
[12] Ameri T, Dennler G, Lungenschmied C and Brabec C J 2009 *Energy Environ. Sci.* **2** 347
[13] Zhao D, Sun X, Jiang C, Kyaw A, Lo G and Kwong D 2008 *Appl. Phys. Lett.* **93** 083305
[14] Kim J Y, Lee K, Coates N E, Moses D, Nguyen T Q, Dante M and Heeger A J 2007 *Science* **317** 222
[15] Gilot J, Wienk M M and Janssen R A J 2007 *Appl. Phys. Lett.* **90** 143512
[16] Sun X W, Zhao D W, Ke L, Kyaw A K K, Lo G Q and Kwong D L 2010 *Appl. Phys. Lett.* **97** 053303
[17] Chou C H, Kwan W L, Hong Z, Chen L M and Yang Y 2011 *Adv. Mater.* **23** 1282
[18] Kouijzer S, Esiner S, Frijters C H, Turbiez M, Wienk M M and Janssen R A J 2012 *Adv. Energy Mater.* **2** 945
[19] You J, Dou L, Yoshimura K, Kato T, Ohya K, Moriarty T, Emery K, Chen C, Gao J and Li G 2013 *Nat. Commun.* **4** 1446
[20] De Jong M, Van Ijzendoorn L and De Voigt M 2000 *Appl. Phys. Lett.* **77** 2255
[21] Krebs F C and Norrman K 2007 *Prog. Photovoltaics* **15** 697
[22] Jørgensen M, Norrman K and Krebs F C 2008 *Sol. Energy Mater. Sol. Cells* **92** 686
[23] Voroshazi E, Verreet B, Aernouts T and Heremans P 2011 *Sol. Energy Mater. Sol. Cells* **95** 1303
[24] Xu Z, Chen L M, Yang G, Huang C H, Hou J, Wu Y, Li G, Hsu C S and Yang Y 2009 *Adv. Funct. Mater.* **19** 1227
[25] White M, Olson D, Shaheen S, Kopidakis N and Ginley D S 2006 *Appl. Phys. Lett.* **89** 143517
[26] Waldauf C, Morana M, Denk P, Schilinsky P, Coakley K, Choulis S and Brabec C 2006 *Appl. Phys. Lett.* **89** 233517
[27] Hau S K, Yip H L, Baek N S, Zou J, O'Malley K and Jen A K Y 2008 *Appl. Phys. Lett.* **92** 253301
[28] Yang T, Cai W, Qin D, Wang E, Lan L, Gong X, Peng J and Cao Y 2010 *J. Phys. Chem. C* **114** 6849
[29] Sun Y, Seo J H, Takacs C J, Seifter J and Heeger A J 2011 *Adv. Mater.* **23** 1679
[30] Kyaw A, Sun X, Jiang C, Lo G, Zhao D and Kwong D 2008 *Appl. Phys. Lett.* **93** 221107
[31] Gevaerts V S, Furlan A, Wienk M M, Turbiez M and Janssen R A J 2012 *Adv. Mater.* **24** 2130
[32] Beek W J E, Wienk M M, Kemerink M and Yang X 2005 *J. Phys. Chem. B* **109** 9505
[33] Zhao D, Liu P, Sun X, Tan S, Ke L and Kyaw A 2009 *Appl. Phys. Lett.* **95** 153304
[34] Sista S, Park M H, Hong Z, Wu Y, Hou J, Kwan W L, Li G and Yang Y 2009 *Adv. Mater.* **22** 380
[35] Chen F C and Lin C H 2009 *J. Phys. D* **43** 025104
[36] Kim S S, Na S I, Jo J, Kim D Y and Nah Y C 2008 *Appl. Phys. Lett.* **93** 073307
[37] Hau S K, Yip H L, Chen K S, Zou J and Jen A K Y 2010 *Appl. Phys. Lett.* **97** 253307
[38] Kumar A, Sista S and Yang Y 2009 *J. Appl. Phys.* **105** 094512